INTERNATIONAL JOURNAL FOR NUMERICAL METHODS IN FLUIDS
Int. J. Numer. Meth. Fluids 0000; **00**:1–13
Published online in Wiley InterScience (www.interscience.wiley.com). DOI: 10.1002/fld

Stabilization of the 3-D spherical convection code Terra

Markus Müller, Christoph Köstler

Received . . .

1. INTRODUCTION

We first shortly describe the application range of our simulation code as it broadened during its development - using numerical improvements and imposing new challenges - and then compare it to present day alternative approaches from a numerical point of view. We then outline the technical improvements described in the paper.

1.1. Modeling Convection and Evolution of the Earth's Mantle Using Terra

One of the earliest three-dimensional numerical models of mantle convection was the spherical-shell model Terra, developed by John Baumgardner [1, 2]. It uses a finite-element discretization on a pentahedral grid (prisms with spherical triangles as top and bottom faces), and it utilizes an efficient multigrid algorithm to solve for the velocity. It was parallelized by Bunge and Baumgardner [3] through message passing and lateral domain decomposition in two of three dimensions. A first study of convection with Earth-like Rayleigh number of 10^8 and depth-dependent viscosity was done by Bunge, Richards and Baumgardner [4]. At the same time, Yang [5] improved the multigrid algorithm with matrix-dependent transfer operators to represent varying viscosity properly . With this code, Richards [6] investigated surface mobility as a function of viscosity variation and yield stress, and Reese [7] explored a parameter range of $\Delta\eta$ between 10^5 and 5×10^7 with an internal Rayleigh number of 10^6. Based on postglacial rebound, mantle mineralogy, seismic tomography, thermodynamics and high-pressure geophysics, Walzer [8] derived a viscosity profile with three high-viscosity and three low-viscosity zones and steep gradients. Even though this model had to be restricted especially regarding lateral variations of viscosity due to temperature-dependence, which it has not yet been possible to resolve numerically, they were able to reproduce the evolution of self-consistent oceanic plates in connection with the thermal evolution of the the Earth. More recently Walzer [9, 10] showed the importance of these viscosity variations for plate tectonics and surface mobility on Earth and incorporated chemical differentiation of continents and, as a complement, of the depleted MORB mantle (DMM). In their model, continents evolve by the interplay of chemical differentiation and convection/mixing, without the requirement of modified boundary conditions on the outer surface of the shell. DMM is partly stirred into the other mantle reservoirs, resulting in a marble-cake mantle with a high concentration of DMM in the asthenosphere [11]. Terra was also applied by Oldham [12] to investigate layered convection and by Bunge and Davies [13–16] to study thermally driven mantle plumes. To reach a higher grid resolution in the upper mantle, Davies [17] added a multi-resolution multigrid method to Terra.

Phillips and Coltice [18–22] studied the influence of mobile continents on mantle temperature and convective wavelength.

Bunge [23] used Terra to calculate mantle flow in a circulation model to further constrain seismic tomographic imaging of the mantle. They further did inverse modeling with data assimilation for the

Copyright © 0000 John Wiley & Sons, Ltd.

past 200 Ma [24, 25] to infer mantle flow and structure from seismic tomography and plate motion history. Schuberth [26,27] also investigated thermal and elastic properties and heterogeneities within the mantle to explain velocity models based on global seismic tomography.

Iaffaldano [28] coupled Terra to a lithospheric model to study plate coupling at the Nazca-South America convergent margin.

1.2. Numerical Methods

Stable Stokes solvers as parts of simulations of convection in planetary mantles are not yet standard. There is a reasonable number of codes using nearly as many numerical approaches. Early examples of finite difference (FD) methods are the codes of Ratcliff and Yoshida [29,30] which use a latitude-longitude grid. Many other FD models connect several patches of nearly orthogonal grids to a global spherical grid, either non-overlapping [31, 32] or even overlapping patches [33, 34]. Some [35, 36] use finite volume (FV) approaches. Beside our own model [2, 37] some other codes [32, 38] use finite elements (FE).

While it is hopeless to try to prove numerical stability for the different FD approaches, theory exists to handle the FV and FE cases. However, whereas the FV methods mentioned above are proved to be stable by the theory, this is not true for most of the FE approaches which *all* use unstable finite element pairs.

Although the violation of the LBB stability condition by low-order velocity-pressure pairs has been known since 1974 [39], they still have been the method of choice for many applications. Their attraction arising from the simple data structures, the moderate size of the arising algebraic problems and low bandwidth even in three dimensions often seems to compensate the additional effort generated by the need to stabilize the arising linear systems subsequently or post-process the data. Fortunately, the question of stability has recently gained attention from the mantle-convection community so that the need for stabilization is eventually addressed. Accordingly, [38] who use a unstable $Q_1 - Q_1$ discretization apply a polynomial pressure stabilization. Another available and widely used FE code [32] still uses an unstabilized $Q_1 - P_0$ discretization and tries to circumvent some of the effects of it's inf-sup deficiency with a penalty method. The same verdict unfortunately holds for the Terra code we have been using for several years. There is no proof of its stability for the Stokes system, which is furthermore not to be expected for the basic finite element pair since an equal-order interpolation is used.

This paper describes how this shortcoming is repaired with a stabilization method. A brief overview of the variety of availabe stabilization approaches including a new one is given in [40], a more detailed in [41]. The new approach is appealing because it requires neither the computation of derivatives, mesh-dependent parameters nor the introduction of nonstandard data structures and leads to symmetric matrices. These properties render it very appropriate for the implementation in an already existing code. However, there is one obstacle to overcome which consists in the nonstandard FE defined on Terra's nonstandard grid. The latter is based on an icosahedral triangulation of the sphere [2, 37] (see 1.4). The same grid is also widely used in oceanography [42] and weather forecast [43] and is well suited to finite elements.

The remainder of the paper proves that it also meets the requirements of the stabilization method [40] and is structured as follows: In Section 1.5 we give a brief overview of the used finite element spaces and the nomenclature used throughout the paper. The material needed to show the desired stability is presented in Section 2. The proof of stability will be given in Section 3. In Section 2.1 we outline the essential steps according to [40] and mark the alterations to essential lemmata required by our 3-D spherical elements whose proofs will be subsequently given in chapter 2.2.

1.3. Governing Equations

The mathematical formulation of convection in the Earth's mantle consists of a (generalized) Stokes equation system for velocity and pressure, supplemented by an energy equation, an equation of state and a set of boundary conditions. With respect to stability we only consider the Stokes system. It

Copyright © 0000 John Wiley & Sons, Ltd.

Prepared using fldauth.cls
DOI: 10.1002/fld

comprises the conservation equations for momentum and mass.

$$-\nabla \cdot \tau + \nabla p = \rho \mathbf{g} \quad (1)$$

$$\frac{\partial \rho}{\partial t} + \nabla \cdot (\rho \mathbf{u}) = 0, \quad (2)$$

where $\mathbf{u}$ is the velocity, p pressure, ρ density, $\mathbf{g}$ gravity and τ the deviatoric shear stress tensor. In the momentum equation (1), $\mathbf{u}$ is included implicitly through τ.

Most regions of the mantle are characterized by linear rheology, thus it is a special case of the model. Then the stress tensor is related to strain rate, $\dot{\varepsilon}$, by

$$\tau_{lm} = 2\eta \left(\dot{\varepsilon}_{lm} - \frac{1}{3} \delta_{lm} \dot{\varepsilon}_{kk} \right) \quad (3)$$

$$= \eta \left(\frac{\partial u_l}{\partial x_m} + \frac{\partial u_m}{\partial x_l} - \frac{2}{3} \delta_{lm} \frac{\partial u_k}{\partial x_k} \right), \quad (4)$$

where η is the dynamic shear viscosity. Because density variations are rather small on a local scale, many models use the Boussinesq-approximation. Then the third summand in (4) vanishes, leading to:

$$\tau_{lm} = \eta \left(\frac{\partial u_l}{\partial x_m} + \frac{\partial u_m}{\partial x_l} \right). \quad (5)$$

Then, with $\rho = const$, the mass equation (2) simplifies to:

$$\nabla \cdot u = 0 \quad (6)$$

The last simplification justifies the common operator notation:

$$A\mathbf{u} + B^T p = \mathbf{f}$$
$$B\mathbf{u} = 0$$

In regard to boundary conditions we restrict ourselves here to the Dirichlet case since our main focus is stability with respect to the grid. It should be mentioned that some of the realistic boundary conditions for mantle convection simulations as e.g. the free slip condition on the spherical surfaces involve additional inf-sup conditions [44, 45]. We also mention that a more detailed analysis of a spatially dependent density further complicates the situation considerably [46] even for standard Dirichlet boundary conditions, let alone the more general situation mentioned above. We also do not consider the from a practical point of view very interesting case of spatially varying viscosity explicitly although the theory is probably applicable without much further difficulties. We mention [47–49] as an example where a continuously differentiable spatially viscosity has been successfully integrated in the theoretical framework. The attempt of a stability proof is however hopeless if the viscosity depends on (dynamic) pressure or nonlinearly on velocity. We cannot consider these general cases here, but try to establish stability at least for the Stokes system, since this is nowadays fortunately considered a fundamental requirement for *any* convection code, e.g. to compute intermediate results correctly that arise from the linearizations of those more realistic models.

1.4. Terra's Grid

Fig. 1 shows a cross-section of the grid currently implemented in Terra as well as a single grid cell. Every such spherical prism T is the image of a reference prism $\hat{T}$ via a mapping $F : \mathbb{R}^3 \mapsto \mathbb{R}^3, F(\hat{T}) = T$. A basis function u on T is then defined as usual via a basis function on the reference prism by $u = \hat{u} \circ F^{-1}$, where $\hat{u}$ is the product of a linear function $\hat{u}_{rad}(z)$ and the linear function $\hat{u}_{lat}(y, x)$ on the triangle that forms the top an bottom faces of the prism. The same basis functions are used for velocity and pressure, thus producing an equal order interpolation.

Copyright © 0000 John Wiley & Sons, Ltd.

Prepared using fldauth.cls
DOI: 10.1002/fld

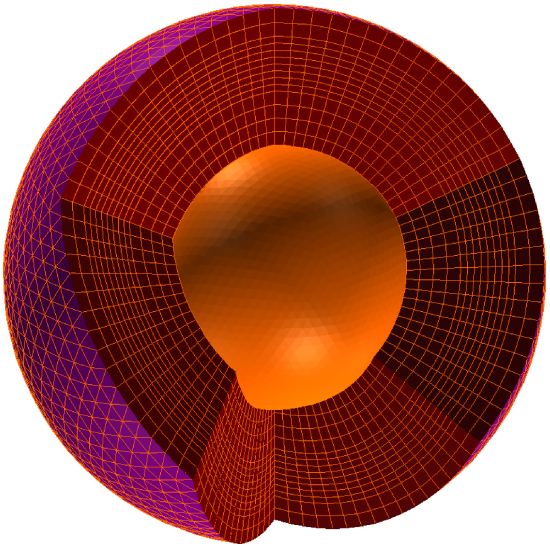

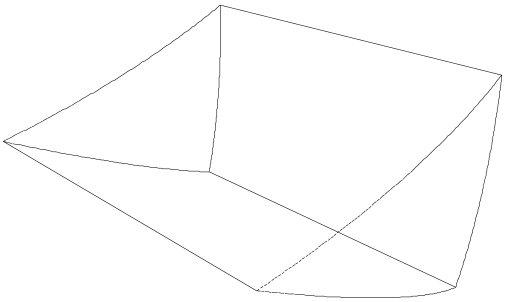

Figure 1. The picture on the left shows a cross-section of Terra's grid, which consists of extruded prisms which spherical top and bottom faces. The basis functions are piecewise bilinear on these prisms.

1.5. Nomenclature

Since we have to recapitulate some results of [40], we will use also the same nomenclature. Ω denotes a simply connected bounded domain in $\mathbb{R}^3$ with a Lipschitz continuous boundary Γ. In our convection code, this is a spherical shell. The standard notation $H^l(\Omega),\ \|\cdot\|_l,\ (\cdot,\cdot)_l,\ l \geq 0$, for the Sobolev spaces of all functions having square integrable derivatives up to order l on Ω is used, and we write $L^2(\Omega)$ instead of $H^0(\Omega)$ and omit the index from the inner product. $H_0^l(\Omega)$ denotes the closure of $C_0^\infty(\Omega)$ with respect to the norm $\|\cdot\|$ and $L_0^2(\Omega)$ the space of square integrable functions with vanishing mean. Spaces consisting of vector valued functions are printed in bold face. The method described in this paper uses finite element spaces for velocity and pressure that are defined with respect to the same partition $\mathcal{T}_h$ of Ω into elements Ω_e In our convection model, Ω_e is a pentahedron or more precisely a spherical prism.

$$R_1 = \{u^h \in C^0(\Omega) | \quad u^h|_{\Omega_e} = u_{lat} u_{rad}\} \tag{7}$$

$$\mathbf{V}^h = \mathbf{R}_1 \cap \mathbf{H}_0^1(\Omega) \quad \text{and} \quad S^h = R_1 \cap L_0^2(\Omega) \tag{8}$$

2. QUOTED PREVIOUS RESULTS

2.1. Stability of the Pressure Correction Method

We want to stabilize a mixed finite element method for the incompressible Stokes equations.

$$A\mathbf{u} + B^T p = \mathbf{f} \tag{9}$$
$$B\mathbf{u} = 0 \tag{10}$$

In variational form this can be described as follows: Seek $(\mathbf{u}, p) \in \mathbf{H}_0^1(\Omega) \times L_2(\Omega)$ such that

$$Q(\mathbf{u}, p; \mathbf{v}, q) = F(\mathbf{v}, q) \qquad \forall (\mathbf{v}, q) \in \mathbf{H}_0^1(\Omega) \times L_2(\Omega) \tag{11}$$

where

$$F(\mathbf{v}) = \int_\Omega \mathbf{f} \cdot \mathbf{v}\, d\Omega \tag{12}$$

Copyright © 0000 John Wiley & Sons, Ltd.
Prepared using fldauth.cls

DOI: 10.1002/fld

$$Q(\mathbf{u},p,\mathbf{v},q) = a(\mathbf{u},\mathbf{v}) + b(\mathbf{v},p) + b(\mathbf{u},q), \tag{13}$$

$$a(\mathbf{u},\mathbf{v}) = \int_\Omega A\mathbf{u}\cdot\mathbf{v}\; d\Omega, \text{ and} \tag{14}$$

$$b(\mathbf{v},p) = -\int_\Omega p\nabla\cdot\mathbf{v}\; d\Omega \tag{15}$$

The mixed variational equation (11) is the first order optimality condition for the saddle-point $(\mathbf{u},p)$ of the Lagrangian functional

$$L(\mathbf{v},q) = \frac{1}{2}a(\mathbf{v},\mathbf{v}) - b(\mathbf{v},q) - F(\mathbf{v}) \tag{16}$$

The restriction of (11) to a pair of finite element subspaces $\mathbf{V}^h \subset \mathbf{H}_0^1(\Omega)$ and $S^h \subset L_0^2(\Omega)$ defines a mixed finite element method which only leads to an accurate solution if the discrete inf-sup condition

$$\sup_{\mathbf{v}^h\in\mathbf{V}^h,\mathbf{v}^h} \frac{b(p^h,\mathbf{v}^h)}{\|\mathbf{v}^h\|} \geq \gamma\|p^h\| \qquad \forall p^h \in S^h \tag{17}$$

with $\gamma > 0$ independent of h is met. This however not the case for equal order finite element approximations including ours. * The method described in [40] aims to lessen this condition by solving a slightly altered problem. The modified Lagrangian additionally includes the pressure projection term $\frac{1}{2}\|(I-\Pi)p\|_0^2$.

$$\tilde{L}(\mathbf{v},q) = \frac{1}{2}a(\mathbf{v},\mathbf{v}) - b(\mathbf{v},q) - F(\mathbf{v}) - \frac{1}{2}\|(I-\Pi)p\|_0^2 \tag{18}$$

where the exact definition of the operator Π depends on S^h. In [40] it is proved that the formulation (18) leads to a stable formulation under the weaker condition of a limited inf-sup deficiency: There exist constants C_1 and C_2 such that.

$$\sup_{\mathbf{v}^h\in\mathbf{V}^h} \frac{\int_\Omega p^h\nabla\cdot\mathbf{v}^h d\Omega}{\|\mathbf{v}^h\|_1} \geq C_1\|p^h\|_0 - C_2 h\|\nabla p^h\|_0 \quad \forall p^h \in S^h \tag{19}$$

and the additional requirement that Π is continuous as an operator $L^2(\Omega) \mapsto L^2(\Omega)$ The authors of [40] then proceed to show that this condition is actually fulfilled for some well known concrete finite element spaces, to this end relying on certain properties of these finite element spaces which are equally well known for those spaces but have to be proved for Terra, accounting for the deviations of our grid from standard finite elements.

To emphasize that we will have to prove that these assumptions hold we state them as lemmata 2.1 and 2.2.

Lemma 2.1 (Bounded interpolation operator)
There exists an operator $I : \mathbf{V} \mapsto \mathbf{V}^h$ such that for the interpolant $I\mathbf{w} = \mathbf{w}^h$ the following ist true:

$$\forall \mathbf{w} \in \mathbf{V} \quad \exists\, \mathbf{w}^h : \quad \|\mathbf{w}^h\|_1 \leq C\|\mathbf{w}\|_1 \tag{20}$$

Remark:
From [51, Lemma 4.1] follows that such an interpolation operator exists for a simplicial finite elements with a polyhedral boundary. The proof in [51] assumes further that there is an affine mapping from the element Ω_e F to a reference element $\tilde{\Omega}_e$ where $F^{-1}(\Omega_e) = \tilde{\Omega}_e$. The estimation

*This can be proved by a general argument described in [50] considering the rank of the matrix M with $m_{i,j} = (\nabla p_i, v_j)$ describing an enclosed flow problem. It n is the number of pressure basis funktions then the rank must be at least $n-1$ to solve the system uniqely (allowing only for an undetermined static pressure offset). This condition can not be fullfilled with our equal order approximation for the sheer lack of velocity basis functions to form a quadratic matrix which is a necessary condition for full rank, or rank $n-1$ in this case.

Copyright © 0000 John Wiley & Sons, Ltd.

Prepared using fldauth.cls
DOI: 10.1002/fld

of the determinant of the affine transformation serves to proof the desired properties. Actually the intersection of the methods treated in [40] and [51] is the P_1 based mixed method. Even for the bilinear Q_1 mentioned ibid. a slightly more detailed analysis would be necessary, since (an isoparametric) mapping F is no longer affine in this case. This is even more true for our pentahedral spherical elements where the mapping F is not even bilinear and thus the needed alterations to [51] would be slightly more complex. However the construction of the operator suggests that (20) can be shown for Q_1 as well as for our spherical elements. We will not do so but rather assume the existence of the desired operator and only give a superficial argument for the plausibility of this assumption. In [51] the mapping F is affine and has the form $F(\tilde{x}) = B\tilde{x} + c$. The derivative DF is then given by B. The proof in [51] poses some requirements to the derivative B of the affine mapping that are equally met by the derivative DF of the mapping that is required for the Q_1 case and also for the more general mapping we will have to use, namely the estimation of its Jacoby determinant, as we will see later. It seems therefore highly probable that somebody has already extended the proof for the Scott-Zhang operator to this slightly more general situation, although we have to admit that we could not find the proper reference up to now. We will nevertheless leave it at this and concentrate on the approximation properties.
The next lemma deals with the approximation property of the finite element space.

Lemma 2.2 (Approximation property)
Let $\mathbf{w}^h$ be the FE interpolation of $\mathbf{w}$. Then $\forall \mathbf{w} \in \mathbf{V} \quad \exists\, \mathbf{w}^h$ such that:

$$\|\mathbf{w} - \mathbf{w}^h\|_0 \leq Ch\|\mathbf{w}\|_1 \tag{21}$$

Since both lemmata 2.1 and 2.2 are well known to hold [†] for the finite element spaces used in [40] the authors can proof the weak inf-sup condition (19) which they later use to proof the stability of the method as mentioned above. We will repeat their argumentes here to be able to point out how the aforementioned lemmata are used. We reproduce and comment the proof in [40] here to show that (20) and (21) are indeed sufficient to establish (19).

According to (8) every $p^h \in S^h$ also belongs to $L^2_0(\Omega)$. From the LBB for the continuous problem we conclude that there exists a $\mathbf{w} \in \mathbf{H}^1_0(\Omega)$ such that

$$\int_\Omega p^h \nabla \cdot \mathbf{w} d\Omega \geq \tilde{C}_1 \|p^h\|_0 \|\mathbf{w}\|_1 \tag{22}$$

From (20) we have

$$\frac{|\int_\Omega p^h \nabla \cdot \mathbf{w}^h d\Omega|}{\|\mathbf{w}^h\|_1} \geq \frac{|\int_\Omega p^h \nabla \cdot \mathbf{w}^h d\Omega|}{C\|\mathbf{w}\|_1} \tag{23}$$

The right-hand side can be further transformed [40]:

$$\begin{aligned}
\frac{|\int_\Omega p^h \nabla \cdot \mathbf{w}^h d\Omega|}{C\|\mathbf{w}\|_1} &= \frac{|\int_\Omega p^h \nabla \cdot (\mathbf{w}^h - \mathbf{w}) d\Omega + \int_\Omega p^h \nabla \cdot \mathbf{w} d\Omega|}{C\|\mathbf{w}\|_1} && (24)\\
&\geq \frac{|\int_\Omega p^h \nabla \cdot (\mathbf{w}^h - \mathbf{w}) d\Omega|}{C\|\mathbf{w}\|_1} + \frac{|\int_\Omega p^h \nabla \cdot \mathbf{w} d\Omega|}{C\|\mathbf{w}\|_1} && (25)\\
&\quad \text{using the triangle inequality} \\
&\geq \frac{\tilde{C}_1}{C}\|p^h\|_0 - \frac{\|\nabla p^h\|_0 \, \|\mathbf{w} - \mathbf{w}^h\|_0}{\|\mathbf{w}\|_1} && (26)\\
&\quad \text{using (22)} \\
&\geq C_1\|p^h\|_0 - C_2 h \|\nabla p^h\|_0 && (27)\\
&\quad \text{using (21)}
\end{aligned}$$

[†] ore reasonably assumed in the case of lemma 2.1 for Q_1

Copyright © 0000 John Wiley & Sons, Ltd.
Prepared using fldauth.cls

DOI: 10.1002/fld

2.2. Specific Approximation Results and Techniques to Generalize them

To derive (21) the authors of [40] use a special case of an approximation result which is well known for simplicial elements [52, p. 217]:

$$\|\mathbf{w} - \mathbf{w}^h\|_0 + h^{1/2}\|\mathbf{w} - \mathbf{w}^h\|_{\Gamma_h} \leq Ch\|\mathbf{w}\|_1 \tag{28}$$

Again the proof of (28) in [52] is based on the determinant of the affine mappings and is not directly applicable. What we need is (21) for *Terra's* grid. We therefore have to dive in a bit further and analyze the procedure used in [52] that is concerned with the proof of this part of the equation. The original lemma reads as follows

$$\inf_{\mathbf{w}_h \in \mathbf{V}_h} \|\mathbf{w} - \mathbf{w_h}\|_{0,h} \leq Ch^k|\mathbf{w}|_k \tag{29}$$

Its proof is divided in two parts witch refer to the two parts of the definition of the norm

$$\|\mathbf{w}_h\|_{0,h} = \left(\|\mathbf{w}_h^2\|_{0,\Omega} + h\|\mathbf{w}_h\|_{0,\Gamma_h}^2\right)^{\frac{1}{2}} \tag{30}$$

The second part of the sum could be handled probably exactly in the same way as in [52] because it is based on a general trace theorem. But fortunately we do not need it because we only rely on (21) The part that has to be adapted is concerned with the approximation quality of the finite element space $\mathbf{V}_h$. We would have to show that

$$\|\mathbf{w}_h\|_{0,\Omega} \leq Ch^k|\mathbf{w}|_{k,\Omega} \qquad \forall \mathbf{w} \in H^k(\Omega) \tag{31}$$

holds. Where in our case $k = 1$ and the situation is much simpler in regard to the order k. The formula then reads:

$$\|\mathbf{w}_h\|_{0,\Omega} \leq Ch|\mathbf{w}|_{1,\Omega} \qquad \forall \mathbf{w} \in H^1(\Omega) \tag{32}$$

Although simpler regarding the order our task is but more general in terms of the admissible mapping. We therefore have to look for situations where nonlinear mappings have been considered. A good starting point are isoparametric finite element spaces for polynomials of order $k > 1$ as e.g. described in [53] and applied to the special case of isoparametrically mapped quadratic triangles ibid. Another one are bilinear mappings of bilinear elements as e.g considered in [52]. We investigated both lines to find a method general enough to handle our situation. According to [53, p. 237] the desired result (31) is usually established in three steps, where the first refers to approximation on the reference element and yields an estimate of the form:

$$|\hat{\mathbf{w}}_h - \mathbf{w}|_{m,q,\hat{T}} \leq C(\hat{T}, \hat{P}, \hat{\Sigma})|\hat{\mathbf{w}}|_{k+1,p,\hat{T}} \tag{33}$$

for some suitable m, k, p, q as defined in [53]. the second one deals with the mapping to an arbitrary grid element, and how the bounds of the seminorms $|v|$ on the grid element are affected by the mapping. The third and final step is the estimation of the parameters of the mapping influencing the seminorms in terms of grid geometry.

Since (unmapped) bilinear prisms are standard finite elements we do not prove here that the first step holds. But we have to discuss steps two and three.

To do so we look at the affine case with $F : \hat{x} \in \hat{T} \mapsto F(\hat{x}) = B\hat{x} + b$ where one gets the following two estimates:

$$|\hat{\mathbf{w}}|_{m,q,\hat{T}} \leq C\|B\|^m|\det B^{-1}|^{1/p}|\mathbf{w}|_{m,q,\hat{T}} \tag{34}$$

$$|\mathbf{w}|_{m,q,\hat{T}} \leq C\|B^{-1}\|^m|\det B|^{1/p}|\hat{\mathbf{w}}|_{m,q,\hat{T}} \tag{35}$$

which for our simple case $k = 0, m = 0, q = 2$ read:

$$|\hat{\mathbf{w}}_h - \mathbf{w}|_{0,\hat{T}} \leq C(\hat{T}, \hat{P}, \hat{\Sigma})|\hat{\mathbf{w}}|_{1,\hat{T}} \tag{36}$$

Copyright © 0000 John Wiley & Sons, Ltd.

Prepared using fldauth.cls
DOI: 10.1002/fld

and (m=1)

$$|\hat{\mathbf{w}}|_{1,\hat{T}} \leq C\|B\||\det B^{-1}|^{1/p}|\mathbf{w}|_{1,\hat{T}} \quad (37)$$

$$|\mathbf{w}|_{1,\hat{T}} \leq C\|B^{-1}\||\det B|^{1/p}|\hat{\mathbf{w}}|_{1,\hat{T}} \quad (38)$$

Then B and $|\det B|$ have to be estimated by the diameter h of the grid cell and the radius of an inscribed ball ρ and there counterparts on the reference cell $\hat{h}$ and $\hat{\rho}$. One gets [53, p. 126]

$$\|B\| \leq h/\hat{\rho} \quad (39)$$

$$\|B^{-1}\| \leq \hat{h}/\rho \quad (40)$$

$$|\det B| = meas(T)/meas(\hat{T}) \quad (41)$$

The task is therefore to find a replacement for B for our slightly more complicated mapping F. which will be based on the derivative of F. To do so we use Theorem 37.1 in [53] which we will give here in its adaption to the case $l = 1, p = 2$

Lemma 2.3
Let Ω and $\hat{\Omega}$ be two bounded open subsets of R^n such that $\Omega = F(\hat{\Omega})$ where F is a sufficiently smooth one-to-one mapping with a sufficiently smooth inverse $F^{-1} : \Omega \mapsto \hat{\Omega}$. Then if a function $\hat{v} : \hat{\Omega} \mapsto R$ belongs to the space $H^1(\hat{\Omega})$, the function $v = \hat{v} \circ F^{-1} : \Omega \mapsto R$ belongs to the space $H^1(\hat{\Omega})$ and, in addition there exist constants C such that

$$|v|_{0,\Omega} \leq |J(F)|^{1/2}_{0,\infty,\hat{\Omega}}|\hat{v}|_{0,\Omega} \qquad \forall \hat{v} \in L^2(\hat{\Omega}), \quad (42)$$

$$|v|_{1,\Omega} \leq C|J(F)|^{1/2}_{0,\infty,\hat{\Omega}}||F^{-1}||_{1,\infty,\Omega}|\hat{v}|_{1,\Omega} \qquad \forall \hat{v} \in H^1(\hat{\Omega}) \quad (43)$$

Where we used the following definitions

$$J(F)(\hat{\mathbf{x}}) = \det(\partial_j F_i(\hat{\mathbf{x}})) = \text{Jacobian of } F \text{ at } \hat{\mathbf{x}} \quad (44)$$

$$||F^{-1}||_{1,\infty,T} = \sup_{\mathbf{x}\in T} \|DF^{-1}(\mathbf{x})\| \quad \mathcal{L}(R^n; R^n) \quad (45)$$

To estimate the $\|DF\|$, $\|DF^{-1}\|$, $J(F)$ and $J^{-1}(F)$ we will follow the two-dimensional example for quadrilaterals given in Lemma A.9 [52, p. 107] and extend it to our needs.

3. ADAPTATIONS TO OUR GRID

3.1. Construction of the Mapping

To show the applicability of Lemma 2.3 we will construct the mapping F and its inverse F^{-1} explicitly. To estimate the quantities for the given grid we will show that F can be represented as product of a bilinear mapping $\tilde{F}$ which fulfills the desired properties and a projecting factor P whose derivative can be shown to be small enough not to interfere with the approximation properties.
Consider an arbitrary gridcell with spherical top and bottom faces. We can approximate this by a pentahedron where these spherical surfaces are replaced by plane triangles. The emerging approximate cell is the image of the reference cell under the bilinear transformation $\tilde{F}$. To write it down explicitly, we introduce the following notation: The triangle nearer the center of the sphere is called the bottom triangle. Its points are given as vectors $\mathbf{B}_a, \mathbf{B}_b, \mathbf{B}_c$ describing the displacement from the center of the sphere. Respectively the points of the top triangle are given by $\mathbf{T}_a, \mathbf{T}_b, \mathbf{T}_c$. and the directional vectors:

$$\mathbf{B}_{ab} = \mathbf{B}_b - \mathbf{B}_a$$

$$\mathbf{B}_{ac} = \mathbf{B}_c - \mathbf{B}_a$$

$$\mathbf{T}_{ab} = \mathbf{T}_b - \mathbf{T}_a$$

$$\mathbf{T}_{ac} = \mathbf{T}_c - \mathbf{T}_a$$

Copyright © 0000 John Wiley & Sons, Ltd.
Prepared using fldauth.cls

DOI: 10.1002/fld

Since the triangles are spherical we have:

$$\begin{aligned} r_B &= |\mathbf{B}_a| = |\mathbf{B}_b| = |\mathbf{B}_c| \\ r_T &= |\mathbf{T}_a| = |\mathbf{T}_b| = |\mathbf{T}_c| \end{aligned}$$

and since the angular components of the spherical coordinates are identical by definition we immediately observe that.

$$\begin{aligned} \mathbf{T}_{ab} &= \frac{r_T}{r_B}\mathbf{B}_{ab} \\ \mathbf{T}_{ac} &= \frac{r_T}{r_B}\mathbf{B}_{ab} \end{aligned}$$

We can now write down the mapping:

$$\tilde{F}(\hat{x},\hat{y},\hat{z}) = \frac{r_T}{r_B}\hat{z}\,(\mathbf{B}_a + \mathbf{B}_{ab}\hat{x} + \mathbf{B}_{ac}\hat{y})$$

We can interpret the real mapping F as its zenithal projection, which is invertible for the angles $\leq \Pi$ and represented here by a projecting factor.

$$\begin{aligned} F &= P\tilde{F} \\ &= \frac{r_B}{|\mathbf{B}_a + \mathbf{B}_{ab}\hat{x} + \mathbf{B}_{ac}\hat{y}|}\tilde{F} \\ &= \frac{r_B}{|\mathbf{B}_a + \mathbf{B}_{ab}\hat{x} + \mathbf{B}_{ac}\hat{y}|}\tilde{F} \end{aligned}$$

3.2. Estimation of the Mapping

We now compute and estimate the derivative of F where we will frequently use the regularity of the grid in the sense that the ratio of the radii between the circumscribed ball rho and the diameter and h of a gridcell is bounded and also that r_0 is reasonably large in comparison to h which means that we keep well away from the center of the sphere. All these assumptions are definitely true for all our applications of the grid. We therefore drop ρ altogether in favor of Ch.

$$DF = DP\;\tilde{F} + P\;D\tilde{F}$$

We consider first the norm of the derivative of $\tilde{F}$ which is obviously a linear function. Its maxima are therefore attained at the vertices, and which can therefore easily estimated by $\|D\tilde{F}\| < Ch$ whereas $\|\tilde{F} < ch^2\|$. Expanding $\|P\|$ into a series shows that $\|P\| < 1 + C\frac{h^2}{r_0{}^2}$. It remains to estimate the norm of the derivative of P for which we get $\|DP\| < \frac{ch}{\sqrt{r_0}}$ We therefore have the desired result:

$$\|DF\| < Ch$$

Now we consider the Jacobian

$$J_F(\hat{x},\hat{y},\hat{z}) = \det(D_F(\hat{x},\hat{y},\hat{z}) < Ch^3$$

because the determinant in R^3 is a trilinear functional.
Since $D(F^{-1} \circ F = (DF)^T)^{-1}$ and $J_{F^{-1}} \circ F = \frac{1}{J_F}$ we also have

$$\begin{aligned} \|DF^{-1}\|_\infty &\leq C\frac{1}{h} \\ \|J_{F^{-1}}\|_\infty &\leq C\frac{1}{h^3} \end{aligned}$$

We now use these results to estimate the approximation properties in the way it has been done in [52, Lemma A.9 p. 107]. Please note two deviations from the original situation.

Copyright © 0000 John Wiley & Sons, Ltd.
Prepared using fldauth.cls

DOI: 10.1002/fld

1. Our special case is much simpler than the general case of higher order elements treated there. While polynomials in Q_k do necessitate a different semi-norm due to mixed derivatives if $k > 1$ the latter do not arise for the case $k = 1$ which we are interested in.
2. Since we are concerned with a three-dimensional problem the Jacobian is $O(h^3)$ where it would be $O(h^2)$ in the two dimensional case, to which [52] refers.

We therefor have the following much less general version of the aforementioned lemma, adapted to the three-dimensional case.

$$\begin{aligned} |v|_{0,p,K} &\leq C_1 h^{\frac{3}{p}} |\hat{v}|_{0,p,\hat{K}} \\ |\hat{v}|_{1,p,\hat{k}} &\leq C_3 h_k^{-\frac{1}{p}} |v|_{1,p,k} \end{aligned}$$

Where we recognize the reappearance of the estimates for the Jacobian J_f in the first and of DF^{-1} in the second equation. The desired approximation property for our grid will be again a much less general form of Corollary A.5 in [52, p. 107]. To state it we have to give some definitions before.

Let $p = q$ and consider the operator

$$\hat{I} \in \mathcal{L}(H_p^1(\hat{K}); H_p^1(\hat{K})) : \hat{I}(t) = t \quad \forall t \in Q_k$$

and define its counterpart I by

$$Iv \in \mathcal{L}(H_p^1(K); H_p^1(K)) : \widehat{Iv} = \quad \hat{I}\hat{v}$$

Let furthermore the "triangulation" $\mathcal{T}_h$ be regular. Then we have:

$$|v - I|_{1,p,K} \leq Ch|v|_{1,p,K} \tag{46}$$

3.3. Theoretical Summary

Eq. (46) is a more general formulation of (21). Under the reasonable assumption that an interpolation operator fulfilling (20) can be actually constructed according to [51] (19) holds for our grid and the code can be stabilized by the pressure correction method.

Actually this is not surprising but had been suggested by the fact that our grid differs only very little from the bilinear grid that is its limiting case.

The presented analysis however shows *which* ingredients are needed to prove it, namely the approximation property, and *how* they can be shown through the concrete definition of the mapping Terras grid, which had not been analysed in detail before.

4. IMPLEMENTATION AND NUMERICAL RESULTS

4.1. Implementation

The implementation of the application of the operator Π in (18) is straightforward and described in [55]. It produces an additional block matrix $-C$ in the Stokes system :

$$\begin{bmatrix} A & B^T \\ B & -C \end{bmatrix} \begin{bmatrix} \mathbf{v} \\ p \end{bmatrix} = \begin{bmatrix} \mathbf{f} \\ g \end{bmatrix}$$

where C is the sum of element-wise stabilization matrices which can be assembled locally from integrals of the finite element base functions. The only grid-specific part are base functions ψ_i and ψ_j .

$$c_{e-ij} = \frac{1}{\nu_e} \left[\int_{\Omega_e} \psi_i(\mathbf{x}) \psi_j(\mathbf{x}) d\Omega - \frac{1}{|\Omega_e|} \int_{\Omega_e} \psi_i(\mathbf{x}) d\Omega \int_{\Omega_e} \psi_j(\mathbf{x}) d\Omega \right] \qquad \forall \Omega_e \in T_h$$

Copyright © 0000 John Wiley & Sons, Ltd.

Prepared using fldauth.cls
DOI: 10.1002/fld

where ν_e denotes the cell averaged viscosity, so that

$$C_{ij} = \sum_{\Omega_e : \Omega_e \subset supp(\psi_i) \cup supp(\psi_j)} c_{e-ij}$$

A more thorough discussion of implementational details including the feedback to the choice of appropriate solvers is given in an already submitted paper [56].

4.2. Numerical Results

From our point of view it would be desirable to have a direct comparison between the accuracy of the new method compared to the old one that shows the supremacy of the new approach. We do not have such a testcase though. Since we do not know of any analytical test case for convection in a spherical shell it is hard to prove a reduction of the overall *error* exactly. The next thing to do is to use a numerically determined solution as a reference, preferably obtained with the help of a code that is stable in the sense of the LBB. Such a comparison has been part of the standard test suite for Terra for some time. In this benchmark a stationary solution for a symmetric convection field with three plumes triggered by a spherical harmonic temperature field at the core-mantle boundary is computed and parameters of the evolving flow are compared with the result that could be also reproduced with other mantle convection codes including the (stable) FV formulation of [35] The benchmark including a discussion of the reasons that lead to the choice of the controlled parameters is described in detail in an important paper [36]. The interesting question is how the stabilized Terra performed in this situation.

The new version of the code has been successfully applied to the benchmark case, as had the ustabilized version before that. The same thing happens to the other regression test cases that compare Terra every new version of the code to previous ones. While this takes some drama from the results of this paper it lends credibility to the old versions of Terra. This is by the way totally consistent with the somewhat subtle theory behind the LBB. i Although the equal order interpolation that had been formally used can even be prooved to be unstable with tha aforementioned counting of degrees of freedom, the vector space of possible spurious pressure oscillations S is generally not known beforehand even though for some unstable pairs such patterns have been found. Concludingly a method whose stability in terms of the LBB is questionable (as is the case for the previous versions of Terra) is not *bound* to reveal this unstability in numerical results, since one can not induce an error known to be unvisible to the equal order interpolation and observe it being taken care of by the stabilized method, if one does not know a basis of S to construct the error. Our numerical results up to now therefor suggest that we have avoided a possible source of error, without that error having actually popped up in the testcases before.

5. CONCLUSIONS AND OUTLOOK

The numerical stability of convection simulation in planetary mantles is crucial for the reliability of the results but has gained recognition only lately. The application of the pressure-polynomial stabilization eliminates one extremely dangerous source of instability by showing that the incompressible Stokes system as a very important special case of mantle-convection simulations can be solved correctly with the stabilized version of Terra.

REFERENCES

1. Baumgardner JR. A three-dimensional finite element model for mantle convection. PhD Thesis, Univ. of California, Los Angeles 1983.
2. Baumgardner JR. Three-dimensional treatment of convective flow in the Earth's mantle. *Journal of Statistical Physics* 1985; **39**:501–511.
3. Bunge HP, Baumgardner JR. Mantle convection modelling on parallel virtual machines. *Computers in Physics* 1995; **9**:207–215.

Copyright © 0000 John Wiley & Sons, Ltd.
Prepared using fldauth.cls

DOI: 10.1002/fld

4. Bunge HP, Richards MA, Baumgardner JR. A sensitivity study of three-dimensional spherical mantle convection at 10^8 Rayleigh number: Effects of depth-dependent viscosity, heating mode and an endothermic phase change. *J. Geophys. Res.* 1997; **102**:11 991–12 007.
5. Yang WS. Variable viscosity thermal convection at infinite prandtl number in a thick spherical shell. PhD Thesis, University of Illinois, Urbana-Champaign 1997.
6. Richards MA, Yang WS, Baumgardner JR, Bunge HP. Role of a low-viscosity zone in stabilizing plate tectonics: Implications for comparative terrestrial planetology. *Geochem. Geophys. Geosys.* 2001; **3**:1040, doi: 10.1029/2000GC000115.
7. Reese CC, Solomatov VS, Baumgardner JR. Scaling laws for time-dependent stagnant lid convection in a spherical shell. *Phys. Earth Planet. Int.* 2005; **149**:361–370.
8. Walzer U, Hendel R, Baumgardner J. The effects of a variation of the radial viscosity profile on mantle evolution. *Tectonophysics* 2004; **384**:55–90.
9. Walzer U, Hendel R. Mantle convection and evolution with growing continents. *J. Geophys. Res.* 2008; **113**:B09 405, doi:10.1029/2007JB005459.
10. Walzer U, Hendel R. Predictability of Rayleigh-number and continental-growth evolution of a dynamic model of the Earth's mantle. *High Perf. Comp. Sci. Engng. Garching/Munich '07*, Wagner S, M Steinmetz AB, MBrehm (eds.). Springer: Berlin, 2009; 585–600.
11. Walzer U, Hendel R. A geodynamic model of the evolution of the Earth's chemical mantle reservoirs. *High Perf. Comp. Sci. Engng. Stuttgart '10*, Nagel WE, Kröner DB, Resch MM (eds.). Springer: Berlin, 2011; 573–592.
12. Oldham D, Davies JH. Numerical investigation of layered convection in a three-dimensional shell with application to planetary mantles. *Geochem. Geophys. Geosys.* 2004; **5**:Q12C04.
13. Bunge HP. Low plume excess temperature and high core heat flux inferred from non-adiabatic geotherms in internally heated mantle circulation models. *Phys. Earth Planet. Int.* 2005; **153**:3–10.
14. Davies JH, Bunge HP. Are splash plumes the origin of minor hotspots? *Geology* 2006; **34**:349–352.
15. Davies JH. Steady plumes produced by downwellings in earth-like vigor spherical whole mantle convection models. *Geochem. Geophys. Geosys.* 2005; **6**:Q12 001.
16. Davies DR, Davies JH. Thermally-driven mantle plumes reconcile multiple hot-spot observations. *Earth Planet. Sci. Lett.* 2009; **278**(1-2):50–54.
17. Davies DR. Applying multi-resolution numerical methods to geodynamics. PhD Thesis, Univ. Cardiff 2008.
18. Phillips BR, Bunge HP. Heterogeneity and time dependence in 3D spherical mantle convection with continental drift. *Earth Planet. Sci. Lett.* 2005; **233**:121–135.
19. Phillips BR, Bunge HP. Supercontinent cycles disrupted by strong mantle plumes. *Geology* 2007; **35**:847–850, doi:10.1130/G23686A.1.
20. Coltice N, Phillips BR, Bertrand H, Ricard Y, Rey P. Global warming of the mantle at the origin of flood basalts over supercontinents. *Geology* 2007; **35**:391–394.
21. Phillips B, Bunge HP, Schaber K. True polar wander in mantle convection models with multiple, mobile continents. *Gondw. Res.* 2009; **15**:288–296.
22. Phillips BR, Coltice N. Temperature beneath continents as a function of continental cover and convective wavelength. *J. Geophys. Res.* 2010; **115**:B04 408.
23. Bunge HP, Davies JH. Tomographic images of a mantle circulation model. *Geophys. Res. Lett.* 2001; **28**:77–80.
24. Bunge HP, Richards MA, Baumgardner JR. Mantle-circulation models with sequential data assimilation: Inferring present-day mantle structure from plate-motion histories. *Phil. Trans. Royal Soc. A: Math. Phys. Engng. Sci.* 2002; **360**:2545–2567.
25. Bunge HP, Hagelberg CR, Travis BJ. Mantle circulation models with variational data assimilation: Inferring past mantle flow and structure from plate motion histories and seismic tomography. *Geophys. J. Int.* 2003; **152**(2):280–301, doi:10.1046/j.1365-246X.2003.01823.x.
26. Schuberth BSA, Bunge HP, Steinle-Neumann G, Moder C, Oeser J. Thermal versus elastic heterogeneity in high-resolution mantle circulation models with pyrolite composition: High plume excess temperatures in the lowermost mantle. *Geochem. Geophys. Geosys.* 2009; **10**(1).
27. Schuberth BSA, Bunge HP, Ritsema J. Tomographic filtering of high-resolution mantle circulation models: Can seismic heterogeneity be explained by temperature alone? *Geochem. Geophys. Geosys.* 2009; **10**(5).
28. Iaffaldano G, Bunge HP, Bücker M. Mountain belt growth inferred from histories of past plate convergence: A new tectonic inverse problem. *Earth Planet. Sci. Lett.* 2007; **260**:516–523.
29. Ratcliff JT, Schubert G, Zebib A. Three-dimensional variable viscosity convection of an infinite Prandtl Number Boussinesq fluid in a spherical shell. *Geophys. Res. Lett.* 1995; **22**:2227–2230.
30. Yoshida M, Iwase Y, Honda S. Generation of plumes under a localized high viscosity lid in 3-d spherical shell convection. *Geophys. Res. Lett.* 1999; **26**:947–950.
31. Zhong S, Zuber M, Moresi L, Gurnis M. Role of temperature-dependent viscosity and surface plates in spherical shell models of mantle convection. *J. Geophys. Res.* 2000; **105**:11 063–11 082.
32. Zhong SJ, Yuen DA, Moresi LN. Numerical methods in mantle convection. *Treatise on Geophysics, Vol. 7: Mantle Dynamics*, Bercovici D (ed.). Elsevier, 2007; 227–252.
33. Yoshida M, Kageyama A. Low-degree mantle convection with strongly temperature- and depth-dependent viscosity in a three-dimensional spherical shell. *J. Geophys. Res.* 2006; **111**:B03 412, doi:10.1029/2005JB003905.
34. Tackley PJ. Modelling compressible mantle convection with large viscosity contrasts in a three-dimensional spherical shell using the yin-yang grid. *Phys. Earth Planet. Int.* 2008; **171**:7–18.
35. Harder H, Hansen U. A finite-volume solution method for thermal convection and dynamo problems in spherical shells. *Geophys. J. Int.* 2005; **161**:522–532.
36. Stemmer K, Harder H, Hansen U. A new method to simulate convection with strongly temperature- and pressure-dependent viscosity in a spherical shell: Applications to the Earth's mantle. *Phys. Earth Planet. Int.* 2006; **157**:223–249.

Copyright © 0000 John Wiley & Sons, Ltd.
Prepared using fldauth.cls

37. Baumgardner JR, Frederickson PO. Icosahedral discretization of the two-sphere. *SIAM J. Numer. Anal.* 1985; **22**:1107–1115.
38. Burstedde C, Ghattas O, Stadler G, Tu T, Wilcox LC. Parallel scalable adjoint-based adaptive solution of variable-viscosity stokes flow problems. *Computer Methods in Applied Mechanics and Engineering* 2009; **198**(21-26):1691 – 1700, doi:10.1016/j.cma.2008.12.015. Advances in Simulation-Based Engineering Sciences - Honoring J. Tinsley Oden.
39. Brezzi F. On the existence, uniqueness and approximation of saddle-point problems arising from Lagrangian multipliers. *RAIRO Anal. Numer* 1974; **8**(2):129–151.
40. Bochev P, Dohrmann C, Gunzburger M. Stabilization of low-order mixed finite elements for the Stokes equations. *SIAM Journal on Numerical Analysis* 2007; **44**(1):82–101.
41. Barth T, Bochev P, Gunzburger M, Shadid J. A taxonomy of consistently stabilized finite element methods for the Stokes problem. *SIAM Journal on Scientific Computing* 2004; **25**(5):1585–1607.
42. Boal N, Domínguez V, Sayas F. Asymptotic properties of some triangulations of the sphere. *Journal of Computational and Applied Mathematics* 2008; **211**:11–22.
43. Randall D, Ringler T, Heikes R, Jones P, Baumgardner J. Climate modeling with spherical geodesic grids. *Computing in Science & Engineering* 2002; **4**(5):32–41, doi:10.1109/MCISE.2002.1032427.
44. Verfürth R. Finite element approximation of incompressible navier-stokes equations with slip boundary condition. *Numer. Math.* 1987; **50**(6):697–721, doi:http://dx.doi.org/10.1007/BF01398380.
45. Verfürth R. Finite element approximation of incompressible navier-stokes equations with slip boundary condition ii. *Numer. Math.* 1987; **59**(6):615–636.
46. Bernardi C, Laval F, Métivet B, Pernaud-Thomas B. Finite element approximation of viscous flows with varying density. *SIAM Journal on Numerical Analysis* 1992; **29**(5):1203–1243, doi:10.1137/0729073. URL `http://link.aip.org/link/?SNA/29/1203/1`.
47. Tabata M, Suzuki A. A stabilized finite element method for the Rayleigh-Bénard equations with infinite Prandtl number in a spherical shell. *Computer Methods in Applied Mechanics and Engineering* 2000; **190**:387 – 402, doi:10.1016/S0045-7825(00)00209-7.
48. Tabata M, Suzuki A. Mathematical modeling and numerical simulation of Earth's mantle convection. *Lecture Notes in Computational Science and Engineering*, vol. 19, Babuska I, Ciarlet PG, Miyoshi T (eds.). Springer, 2002; 219–232.
49. Tabata M. Finite element approximation to infinite Prandtl number Boussinesq equations with temperature-dependent coefficients–Thermal convection problems in a spherical shell. *Future Generation Computer Systems* 2006; **22**:521–531.
50. Franco Brezzi, Michel Fortin. *Mixed and Hybrid Finite Element Methods*. Springer-Verlag New York, Berlin, Heidelberg, 1991.
51. SCOTT R, Zhang S. Finite element interpolation of nonsmooth functions satisfying boundary conditions. *Mathematics of Computation* 1990; **54**(190):483–493.
52. Vivette Girault, Pierre-Arnaud Raviart. *Finite Element Methods for Navier-Stokes Equations*. Springer-Verlag New York, Berlin, Heidelberg, 1986.
53. Ciarlet P, Lions J, Scott L. Handbook of numerical analysis, volume ii.-finite element methods (part i). *SIAM Review* 1994; **36**(2):320–320.
54. Ciarlet P, Raviart P. Interpolation theory over curved elements, with applications to finite element methods. *Computer Methods in Applied Mechanics and Engineering* 1972; **1**(2):217–249.
55. Dohrmann C, Bochev P. A stabilized finite element method for the Stokes problem based on polynomial pressure projections. *Int. J. Num. Meth. Fluids* 2004; **46**:183–201.
56. Köstler C, Müller M, Walzer U, Baumgardner JB. Krylov solvers and preconditioners for variable-viscosity convection models. *Comp. Geosci.* 2012, submitted; .

Copyright © 0000 John Wiley & Sons, Ltd.
Prepared using fldauth.cls